Biol. Cybern. 61, 103–113 (1989)

Biological Cybernetics

Gabor Filters as Texture Discriminator

I. Fogel[1] and D. Sagi[2]

[1] Department of Atmospheric Optics, Soreq Nuclear Research Center, Yavne 70600, Israel
[2] Department of Applied Mathematics & Computer Sciences, The Weizmann Institute of Science, Rehovot 76100, Israel

Abstract. The present paper presents a model for texture discrimination based on Gabor functions. In this model the Gabor power spectrum of the micropatterns corresponding to different textures is calculated. A function that measures the difference between the spectrum of two micropatterns is introduced and its values are correlated with human performance in preattentive detection tasks. In addition, a two stage algorithm for texture segregation is presented. In the first stage the input image is transformed via Gabor filters into a representation image that allows discrimination between features by means of intensity differences. In the second stage the borders between areas of different textures are found using a Laplacian of Gaussian operator. This algorithm is sensitive to energy differences, rotation and spatial frequency and is insensitive to local translation. The model was tested by means of several simulations and was found to be in good correlation with known psychophysical characteristics as texton based texture segregation and micropattern density sensitivity. However, this simple model fails to predict human performance in discrimination tasks based on differences in the density of "terminators". In this case human performance is better than expected.

1 Introduction

In a number of recent papers (Julesz 1984a, 1986; Treisman 1986) it has been suggested that visual perception operates in two modes, one preattentive and the other attentive. In the preattentive mode (which is parallel), differences in a few local structural features are detected over the entire visual field. In the attentive mode (which is sequential), a serial search over a narrow aperture of attention is performed in fast steps (20–80 ms). Only in this mode recognition is possible. According to the above mentioned works texture segregation in the preattentive mode is based on local feature differences in the picture. Psychophysical experiments (Beck 1972, 1983; Julesz 1975, 1981, 1986) have shown that texture discrimination in the preattentive mode depends mainly on some simple properties such as brightness, color, size and slope (of lines, blobs) of the basic texture elements that compose the picture.

Julesz (1980, 1984a, 1986) has suggested that texture discrimination could be explained in terms of first-order differences between local features called textons, rather than global second-order differences between points in the image as he had suggested before (Julesz 1962). Textons are defined as elongated blobs of specific color, orientation, length and width, along with their terminators and line crossings. Differences in texton densities are necessary for discrimination in the preattentive mode. In a series of experiments Gurnsey and Browse (1987) reported that properties such as terminators and line crossings appear not to play an important functional role in texture discrimination, hence they speculated that they were not textons. They found that performance in texture discrimination tasks depended mainly on *(1)* the particular micropattern pair used, *(2)* which member of the pair forms the foreground and which forms the background, *(3)* the time available to inspect the image and *(4)* the familiarity that the subject has with the patterns and procedure. They suggested that energy differences in the minimal circle enclosing the basic features creating the picture enable discrimination in the preattentive mode. However, they did not suggest that the human visual system computed the minimal enclosing circle for each micropattern in the display: rather, they suggested that when two micropatterns composed of the same line segments are enclosed by different circles, they will stimulate different sets of simple receptors.

Another model was suggested by Krose (1987) who examined the (r, θ) chord space for each micropattern

(texture element) and defined a measure function to measure the dissimilarity between them. (A chord is a virtual line between two pattern points, the chord space is the size and orientation distribution of all those chords, for binary pictures the chord space is identical to the autocorrelation function.) Krose concluded that the use of a local autocorrelation algorithm on binary images in combination with a multi-layer, multi-resolution sampling array plus dissimilarity measure function is a flexible method for the extraction of local structure features. Other models such as Fourier transformation have also been investigated (Bajcsy 1973; Julesz and Caelli 1979).

The model presented here is based on Gabor filters (Gabor 1946; Turner 1986; Caelli and Moraglia 1985; Daugman 1987; Beck et al. 1987). The class of Gabor functions was described by Gabor (1946) and was extended to two dimensions by Daugman (1980, 1987). Daugman showed that Gabor filters are optimal in the sense that they minimize the product of effective areas occupied in the 2-D space and 2-D frequency domains. This class of filters can be described in terms of a sinusoidal plane wave of some spatial frequency and orientation within a two dimensional Gaussian envelope. Beck et al. (1987) suggested that Gabor filters play a role in tripartite segregation and in texture segregation in general. We have chosen Gabor filters because they have properties similar to those of early visual channels, being localized in the space and frequency domains. In addition each filter encodes both spatial frequency and orientation thus predicting preattentive detection of spatial frequency and orientation conjunctions (Sagi 1988). In the first part of this article we apply the Gabor filter model to isolated micropatterns and find the power spectrum of each basic element (by means of Gabor filters) then we calculate the dissimilarity between the two spectra. According to the result of the measure function we decide whether or not the two basic elements are preattentively distinguishable. The calculated measure is compared with data from psychophysical experiments done by Krose (1987). In the second part we describe the Gabor based algorithm for texture segregation (GGL) for textures composed of many micropatterns thus capturing some properties of micropattern groups. A basic assumption we make here is that the only information available for preattentive discrmination is differences between first order statistics of filter responses, computed as spectral energy.

2 Measuring Similarity Using Gabor Filters

A 2-D Gabor function is a harmonic oscillator, which is a sinusoidal plane wave of some frequency and orientation within a Gaussian envelope. Its frequency, orientation and bandwidth are controlled by its parameters. The Gabor function is defined as follows:

$$G(x, y \mid W, \theta, \varphi, X, Y) = \exp^{\frac{-[(x-X)^2+(y-Y)^2]}{2\sigma^2}} \times \sin(W(x\cos\theta - y\sin\theta) + \varphi), \tag{1}$$

where σ is the Gaussian width, θ is the filter orientation, W is its frequency and ϕ is its phase shift. X, Y define the center of the filter. Let $L(x, y)$ be the input element matrix and $G(x, y) \mid W, \theta, \varphi, X, Y)$ the Gabor operator. We find the $G * L$ spectra for various orientations and shifts. This spectrum identifies the texture element. More exactly:

$$\begin{aligned} GL_1(X, Y \mid W, \theta) &= \sum_{xy} G(x, y \mid W, \theta, 0, X, Y) \times L(x, y) \\ GL_2(X, Y \mid W, \theta) &= \sum_{x,y} G(x, y \mid W, \theta, \pi/2, X, Y) \times L(x, y) \\ S^2(X, Y \mid W, \theta) &= GL_1^2(X, Y \mid W, \theta) + GL_2^2(X, Y \mid W, \theta), \end{aligned} \tag{2}$$

where x, y are indices over the basic matrix elements ($x, y = 0, 32$). $\phi_1 = 0$, $\phi_2 = \pi/2$, $W = 2\pi w/17$ where w is the number of cycles in 17 pixels (the size of the input pattern). GL_1, GL_2 are the convolutions of the Gabor filter and the texture. S is the locally shift invariant output of the filters (by means of GL_1 and GL_2). We next introduce a measure function that estimates the level of dissimilarities between the two micropatterns.

The measure function Dtb is defined as follows:

$$D_{tb}^2(W) = \frac{\left| \sum_{X,Y,\theta} S_t^2(X, Y \mid W, \theta) - \sum_{X,Y,\theta} S_b^2(X, Y \mid W, \theta) \right|}{\sum_{X,Y,\theta} S_t^2(X, Y \mid W, \theta) + \sum_{X,Y,\theta} S_b^2(X, Y \mid W, \theta)}, \tag{3}$$

where S_b is the convolution of the first input micropattern (background) with Gabor filter, S_t is the convolution with the second micropattern (target), θ ranges between 0° to 360° in 10° steps, X and Y were varied at steps of σ across a range of 4σ (25 samples). This measure function has values between 0 and 1, and indicates the dissimilarity between the two input micropatterns. These results are invariant to rotation and local shift. If the two input patterns are identical up to rotation and shift within the integration area the result will be small; the higher the dissimilarity between them the closer to 1 the result gets. The integration over different orientations is necessary, since we apply this measure to cases where the patterns are randomly rotated. The integration over spatial positions is due to the uncertainty in pattern position. We integrate filter responses (energy), relying on the assumption that the preattentive system uses only differences of averaged responses and no higher order statistics.

3 Psychophysical Discriminability as a Measure of Similarity

Most of the models for texture discrimination are based on finding local differences in the image. In the present model the local differences are taken into account by the dissimilarity function. We shall show that this model is in high correlation with psychophysical results. For more details about psychophysical experiments see Bergen and Julesz (1983). In brief:

The stimulus containing the target element and many distractors is presented for a short time (20–80 ms) and is followed by a mask constructed from the conjunction of the target and distractor at a variable time (SOA) after the onset of the stimulus. Increase in SOA is expected to increase available stimulus processing time and thus improve performance. Some popular target/distractor pairs are presented in Fig. 1 (from Krose 1986). According to Julesz's texton theory preattentive discrimination is expected in the first pair and attentive discrimination in the second pair. The fifth pair (where the two basic elements have the same number of terminators and line crossing) is preattentively indistinguishable. On the other hand discrimination in the sixth pair is in the preattentive mode since the basic elements differ in four terminators and in line crossing. These pairs were tested by Krose (1987) using experimental procedures as used by Bergen and Julesz (1983). Krose found a high detectability for pairs 6, 1, 4 (ordered by the level of detection) and a low one for pairs 2, 3, 5. These results are only in partial agreement with Julesz's model. Next we shall discuss the performance of our model on these pairs.

3.1 A Single Spatial-Frequency Filter Model

Experiment 1. In this experiment we used simple basic elements (Fig. 1) employed also by Krose (1987) and Julesz (1984b, 1986). All the input elements had the same number of pixels to prevent texture discrimination based on energy differences.

The size of each input micropattern used was 17×17 and it was embedded in a matrix of order 33×33 to allow variations in orientations and shifts.

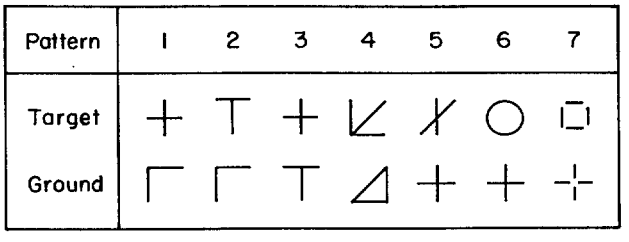

Fig. 1. Combinations of target and distractor micropatterns used in experiment 1. (After Krose 1987)

Table 1. The discriminability results of the micropattern pairs used in experiment 1

Pattern	*Dtb*
1	0.46
2	0.24
3	0.39
4	0.09
5	0.27
6	0.72
7	0.56

Pixels belonging to the basic element will be at gray level 255; other pixels will get the gray value 0. Gabor filter parameters were $\sigma = 8$ and $w = 0.875$ (one cycle for 19 pixels). The input for the model consists of two patterns and the outputs is their dissimilarity. We shall compare these results to those from the human visual system for a fixed SOA. Since we did not introduce the temporal dimension to our model, we chose an arbitrary SOA (240 ms, from Krose 1987).

We calculate S (2) for the two basic elements, as a function of θ and find the distance between the spectra of the convolutions (3). The results of this model are given in Table 1.

The results depicted in Table 1 are in high correlation with the results for the human visual system (Krose 1986, 1987), the discriminability orders of the pairs are almost the same. A comparison between these results is presented in Fig. 2. Note that our model has low performance, compared to the human performance, in the case where the two micropatterns differ in the number of terminators (see Table 1 pair 4).

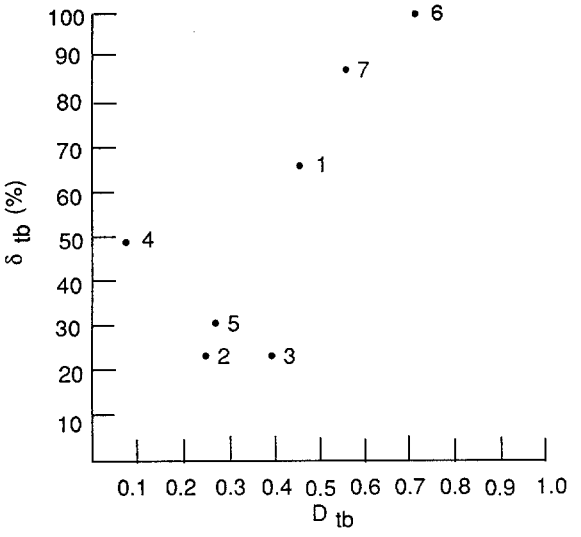

Fig. 2. Correlation between our model predictions ($w = 0.875$) and Krose's psychophysical data, for the patterns shown in Fig. 1

Table 2. The discriminability results of the micropattern pairs used in experiment 2

α (%)	*Dtb*
9	0.21
18	0.33
27	0.39
36	0.42
50	0.46

Experiment 2. Following Krose's experiment, we will find discrimination values for the following pairs: the background elements in this experiment are *L* shapes and the target element vary from *L* to +. See the variation as a function of α in Fig. 3.

All the target elements have the same number of line crossings and terminators. Hence according to the texton theory we expect the discrimination to be the same for all pairs, up to the resolution of crossing detection. Psychophysical results show discriminability variation from 0, where the target is *L*, up to a certain value indicating the discriminability of the (*L*, +) pair, where the target is +. The results of our model are given in Table 2. They are found to be in high correlation with the psychophysical results.

The correlation between the results of the Gabor model with the psychophysical experiments are presented in Fig. 4.

3.2 A Multi Spatial-Frequency Filter Model

In the previous Sect. (3.1) we computed the model discrimination values (in frequency domain) for a single Gabor filter with center frequency of $w=0.875$. However the human visual system contains many filters with different peak spatial frequencies operating in parallel (Wilson 1983; Watson 1983), and it is reasonable to assume that discrimination is based on the filter that yield the best discrimination for the pair of patterns involved. We tested our model on a spatial frequency range of $w=0.5$ to $w=4.25$. For each pattern we selected the filter with the best discrimination value (*Dtb*) and took this value as the discrimination level for the pattern. The results are depicted in Fig. 5. This modified model gives somewhat better fit to the psychophysical data of Krose (1986, 1987) with a correlation coefficient of $r=0.71$. Pattern 4 is again out of range, and may be considered as an exception, without it the correlation coefficient is $r=0.91$. The deviation of patterns 3 and 5 are due to the high spatial frequency components. Limiting the frequency range to $w<1.25$ (highest filter), where most of the patterns energy lies improves correlation up to 0.96. Most discriminability functions have a major peak at w

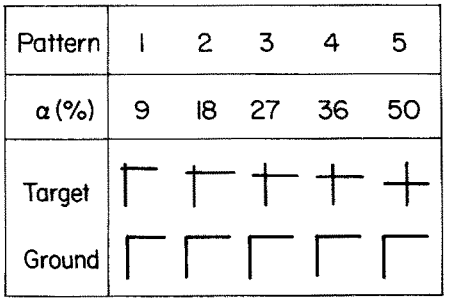

Fig. 3. Combinations of target and distractor micropatterns used in experiment 2. (After Krose 1987)

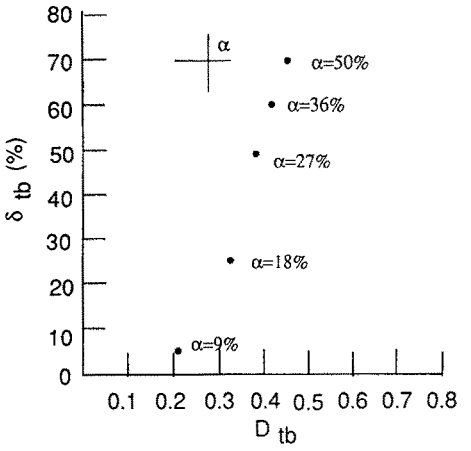

Fig. 4. Correlation between our model predictions ($w=0.875$) and Krose's psychophysical data, for the patterns shown in Fig. 3

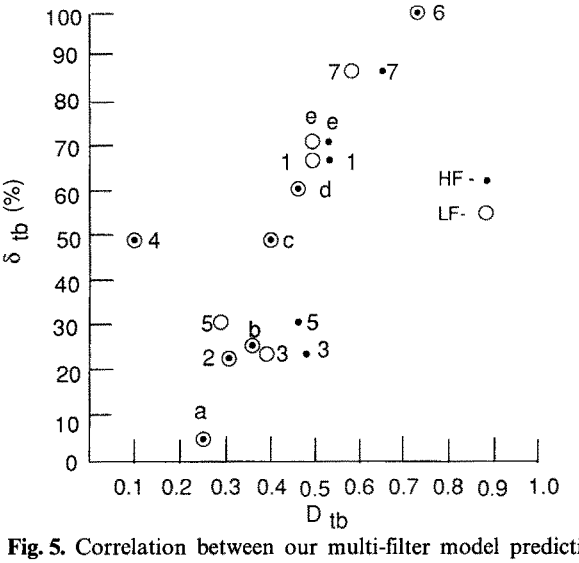

Fig. 5. Correlation between our multi-filter model predictions and Krose's psychophysical data. Textures pairs 1–7 are the same as Fig. 1, pairs *a*–*e* are the same as in Fig. 3. Open symbols are for discriminability values obtained using only low frequency filters ($w<1.25$), solid symbols are for values obtained adding higher frequencies filters ($w<4.25$). The correlation coefficients are $r=0.96$ and $r=0.91$ respectively (without pair 4 and 0.71 with it). Note that *e* and 1 are the same patterns (+, *L*) and the distance between them reflects variations in the psychophysical data

around 0.75 and a secondary one at w around 1.5. Patterns 3 and 5 are significantly better discriminated at $w=1.5$ then at $w=0.75$.

The Gabor filter model, in its present form, cannot account for pattern discrimination based on terminators. Note that for pattern 6, discrimination also may be based on differences in terminators density, and human performance is superior to our model performance (in this case human performance is error free, thus the performance differences may be larger than seen). Thus we may have to modify the Gabor filter model in order to deal with pattern discrimination based on terminators.

3.3 Summary

In the first experiment we tested seven input pairs, where in some of them preattentive discrimination was generated. According to the results of this model the transition from attentive to preattentive mode is gradual throughout the interval between 0 to 1. If a division to preattentive/attentive mode existed we would expect psychophysical data to be close to 100% if the discrimination were preattentive and close to 0% if it were attentive. But the spread of the results implicates that this division is too coarse. Another possibility is that such a division exists and we must add a threshold level to the model above which preattentive mode operates and below which attentive mode is necessary.

The psychophysical performance on the pairs 2 and 3 is almost the same. According to the texton theory, supported by many demonstrations, pair 2 (T, L) is preattentively indistinguishable because texton differences are very low (one terminator), while in the third pair $(T, +)$ preattentive discrimination is possible due to the high texton density differences (one terminator and one line crossing). Introducing a threshold between the two pairs may resolve this problem. Another resolution to this problem comes from the observation that (X, T) discrimination requires high frequency filters while (T, L) and (X, L) discrimination are affected only by low frequency filters. This may result lower sensitivity to (X, T) differences in experiments using short presentation time, due to the longer integration time of high frequency filters (Watson 1983; Wilson 1983).

In the second experiment we held the number of terminators and line crossings constant while varying α (the spatial location of the lines that composes the micropattern, see Fig. 3). The psychophysical and the Gabor model results have changed from close to zero, which means o segregation, up to the level of the detectability of the L, + pair. According to the texton theory texture discrimination should not be greatly affected by increasing α, up to the + resolution.

A quantitative comparison based on correlation coefficients can be made between our model and the local cross – correlation model of Krose (1986, 1987). Taking into account all the patterns used in Sect. 3.2 Krose's model gives a correlation coefficient of 0.65 while ours yields 0.71. Our correlation coefficient can be improved by not considering pair 4 (terminators) up to 0.96, his can be improved by not considering pair 5 up to 0.84 (Krose 1986). The two models fail on different patterns, an observation that may imply that a model combining features from the two models may have a better predictive value. For example, as Krose (1987) points out his model may have better results using the chord space of patterns which are low – pass filtered and then thresholded.

Finally, the model prediction may be affected by the choice of the dissimilarity measure. We took the differences between energies at a particular spatial frequency band as a correlate of discriminability. This was done by integrating over all orientations and is justified since all patterns are randomly rotated. Most pattern pairs, although having the same energy when averaged across all orientations, differ in the distribution of energies across the different orientations (different second order statistics). Krose (1986) used a dissimilarity measure (Euclidean distance) that is sensitive to this differences in some cases. Replacing (3) by the Euclidean distance measure improves our correlation value up to 0.91 (all patterns), mainly due to the improved discriminability on pair 4. It is interesting to note that the energy distribution across the different orientation filters is translated in all stimuli considered here into spatial distribution. This spatial variation may limit discrimination, but on the other hand it can enhance discrimination between textures differing in the second order statistics of the orientation spectrum.

4 Texture Segregation Based on Gabor Filters

The task of the next algorithm (GGL) is to find borders between regions of different textures. This is a subset of the general problem of locating and characterizing different textures. A number of techniques for texture discrimination have been suggested. Most of them limit the number of features and fall into one of the following classes: Template matching (Hall 1979), pattern sampling (Fairhurst and Stonham 1976), spatial transforms, geometrical moments and feature extraction (Rosenfeld and Kak 1976). The algorithm has two stages. In the first stage the input image is transformed into output image by convolution with Gabor signals and enables discrimination between features by means of intensity differences. The target region and the background region will have different intensity levels if they contain different features, hence

they can be segregated easily on this basis. The second stage finds the borders. The algorithm is sensitive to energy differences, rotation and spatial frequency and is insensitive to local translation.

4.1 The GGL Algorithm (Gabor-Gaussian-Laplacian)

A. Convolve the input image with odd and even Gabor filter and compute sum of squares for each position.
B. Smooth the output of *A* (by Gaussian).
C. Threshold.
D. Remove noise (small connected components).
E. Find border lines (by Laplacian).
F. Change parameters in Gabor filter and repeat steps *A–E*.

In the following simulations we used 32 filters having parameters as follows: $\theta = 0°$, 45°, 90°, 135°. $w = 0.5$, 0.625, 0.875, 1. $\varphi = 0°$, 90°. See the filters in Fig. 6.

The parameter σ depends mainly on the input image scale and was tested in the region 6–18, the best choice was 12. There is almost no change in the convolved output around $\sigma = 12$. Phase information is lost by taking only the energy values. The input pictures to this algorithm are of size 512×512 pixels and the graylevel are in the range 0–255, all the pictures are monochrome. We used computer generated images and also images taken by a video camera. Results did not differ in the two cases even though the camera images are noisy in nature. A grid of 32×32 is set on the input image. A convolution with Sine and Cosine Gabor filters of size 65×65 are made around each grid point. Hence the number of output energy values are $(32-4)*(32-4)=784$. The -4 come from the fact that we start at line and column 32 and stop at line and column 480, because the filter integration size is 65×65. For each grid point, the sum of squares of the Sine and Cosine filters outputs is calculated and then transformed into the region 0–255 by means of a linear transformation. The output picture is then a collection of 28×28 squares of 16×16 pixel size, with graylevel distribution depending on the texture used. The edges are computed on each of the convolution outputs (for all θ, ω combinations). As we mentioned earlier the output of the first step is a collection of 28×28 squares. This is a low resolution output. In addition, high graylevel squares may exist in the neighborhood of low graylevel ones and vice versa, this introduces high frequency noise relative to the texture size. For these reasons a smoothing operation is necessary before calculating texture borders. A Gaussian filter of size 31×31 pixels is convolved with the picture in order to smooth it and a threshold is then defined to be in the middle of the two peaks of the smoothed histogram. Since terminators and line crossings can not be trivially converted into Gabor parameters and the basic elements are randomly ordered on the picture (which means variable local density), small connected components (noise) may be occurring. These components are then removed using a connected component algorithm (Rosenfeld and Kak 1976). At the end of this step a binary picture is presented where the graylevels for the discriminable textures are different. Hence by applying a Laplacian operator the borders can be found. The optimal situation is to apply Gabor filter just once. Usually this is not the case and a few application are required. We ran the algorithm a few times varying the Gabor parameters. In the case of no discrimination the output pictures were smooth (no information), and were rejected. In the remaining results we found edges and if they did not differ significantly the average over all of them was taken. Otherwise there is no segregation.

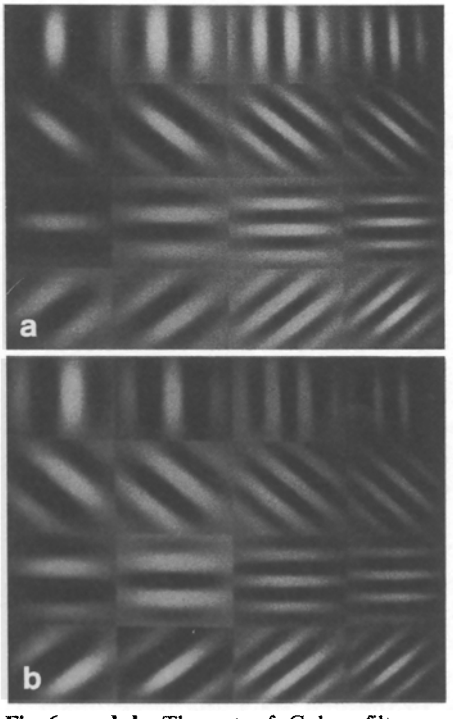

Fig. 6a and b. The set of Gabor filters used in the GGL algorithm. The set contains 4 frequencies (32, 26, 18, and 16 pixels/cycle), 4 orientations (0°, 45°, 90°, 135°) and 2 phase pairs for each orientation and frequency. Variation in frequency along the *X* axis and variation in rotation along the *Y* axis, each figure **(a, b)** has a different phase

4.2 Results

The number of cycles within a Gabor patch increases with σ. Therefore for a fixed σ an optimal region for w can be defined. σ was tested in the region 6–18 and the best choise was 12, 26 pixels per wave period was found

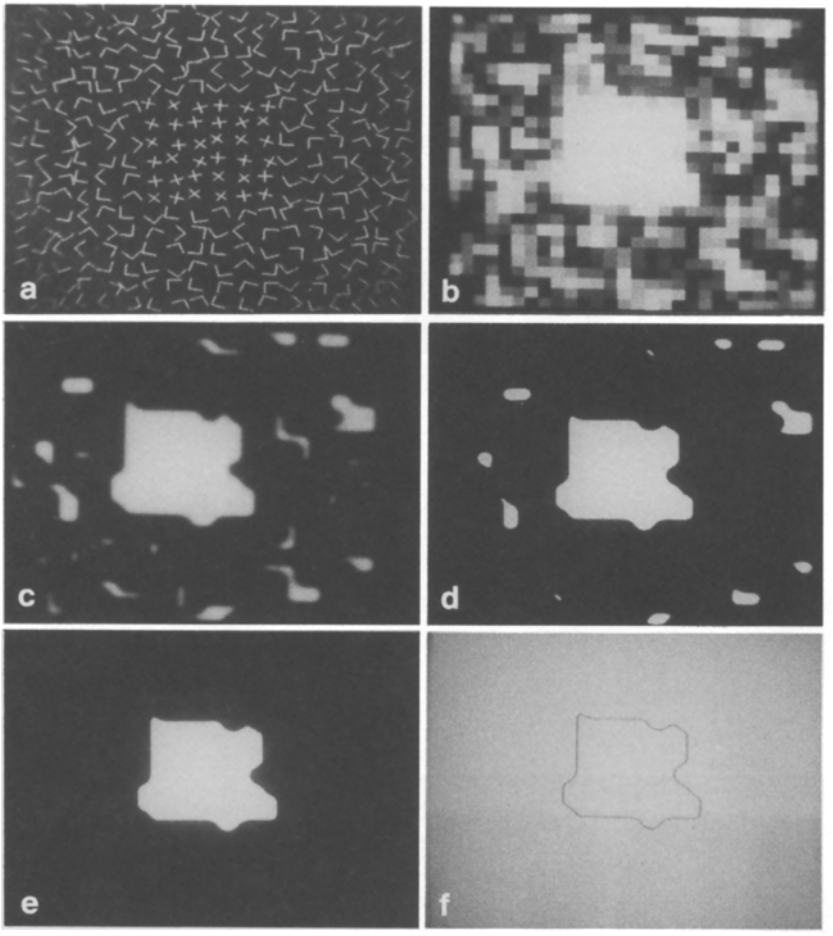

Fig. 7. a The input texture pair: $+s$ embedded in *Ls* distractors. **b** The result of convolving a Gabor filter with the image ($w=0.625$, $\theta=90°$). **c** The smoothing operation (Gaussian) result. **d** The threshold operation result. **e** The result of removing small connected components (noise). **f** The output (Laplacian) result of the GGL algorithm

to be the best choice in most cases (e.g. $w=0.625$ which effectively resembles a DOG function, since for the Gaussian we used there were no effective side bands in addition to the first negatives). In some cases $w=1$ was found to be better than 0.625. So usually it was sufficient to run the algorithm with the parameters $\sigma=12$, $w=0.625$, $\theta=0°$, 45°, 90°. In the following experiments we attempted to discriminate between the different textures and to find the borders between them, using the GGL algorithm. A picture is a combination of two different textures and the basic elements are of size 17×17 pixels randomly (orientation- and translation wise) embedded in a matrix of size 33×33. The textures in the following experiments are a collection of *Ls*, *Os*, *Ts* and $+s$ micropatterns. These micropatterns pairs have been investigated by Bergen and Julesz (1983) and Krose (1987). Bergen and Julesz (1983) found preattentive discrimination for pictures composed of *L* embedded in a background of $35+s$ and attentive discrimination when *L* was embedded in 35 *Ts*. Krose (1987) found high detectability performance for *O* embedded in $+s$. In the first pair (Fig. 7a) which is a collection of $+s$ embedded in a background of *Ls* we found high discriminability between the different textures (Fig. 7b), in addition the borders between them were found (Fig. 7a–f). Almost the same results have been obtained when $+s$ were embedded in *Os* (Fig. 8a–d). Lower segregation was found for $+s$ embedded in *Ts* (Fig. 9a–c) while there was no segregation at all for *Ts* embedded in *Ls* (Fig. 10a–d).

5 General Discussion

In general Gabor functions can easily segregate images having regions differing in one of the following properties: Spatial frequency, density of elements, orientation, phase and energy. The larger the number of differences, the better the separation. These properties can be converted trivially to the Gabor filter parameters. In addition, Gabor filters discriminate well pictures differing in their textons properties except for terminators.

The failure of the Gabor filter based model to predict terminator based discrimination is interesting in itself. Models based on linear filters are quite

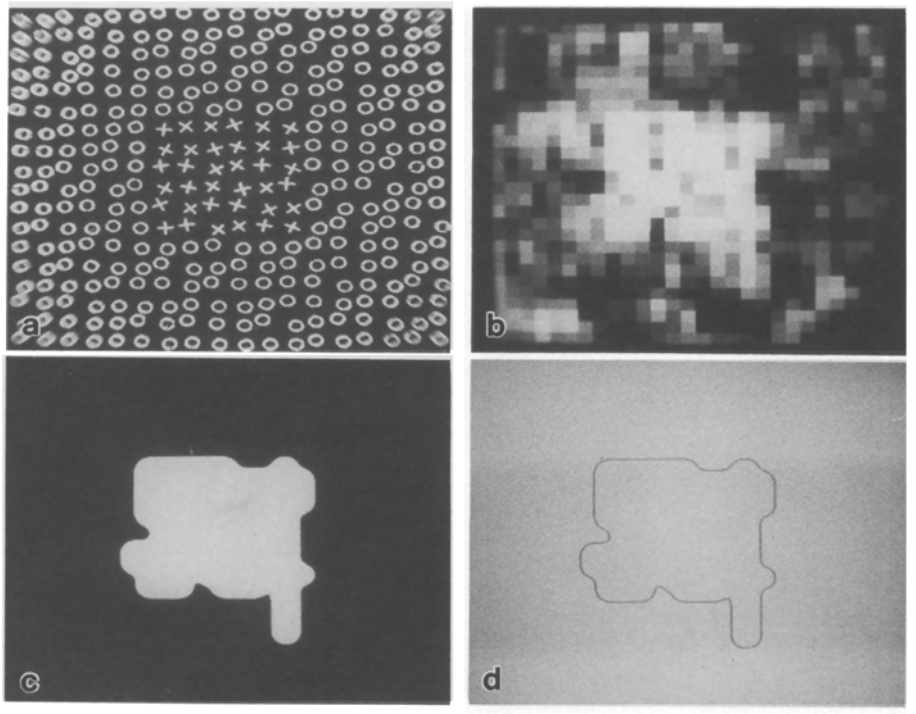

Fig. 8. **a** The input texture pair: $+s$ embedded in Os distractors. **b** The result of convolving a Gabor filter with the image. **c** The result of Gaussian + Threshold + Noise removing. **d** The output (Laplacian) result of the GGL algorithm

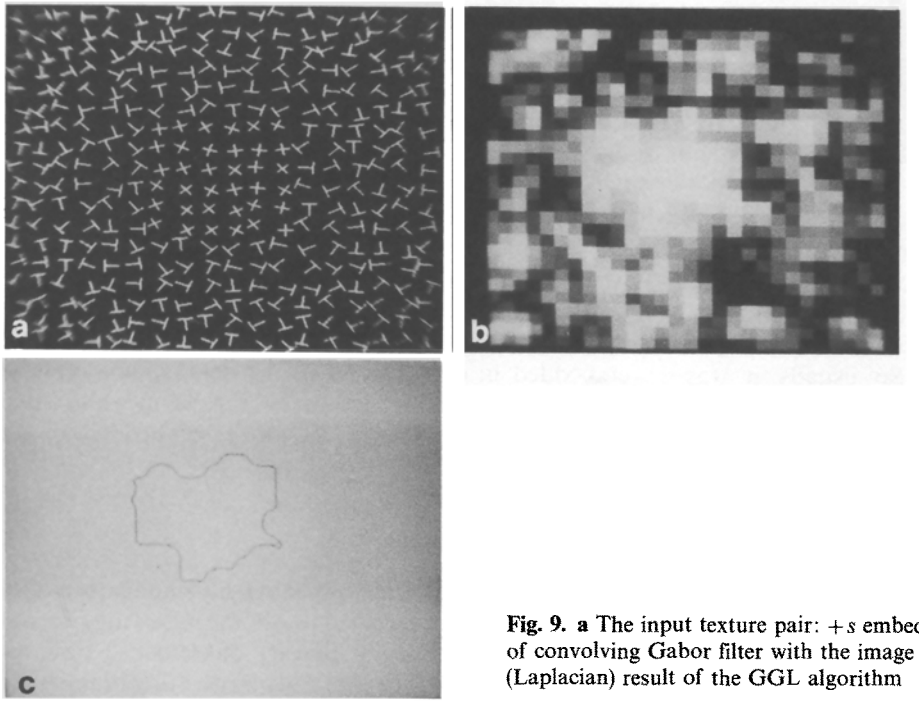

Fig. 9. **a** The input texture pair: $+s$ embedded in Ts distractors. **b** The result of convolving Gabor filter with the image ($w=0.625$, $\theta=90°$). **c** The output (Laplacian) result of the GGL algorithm

successful in predicting visual phenomena, mainly at contrast threshold level (Daugman 1987; Watson 1983; Wilson 1983), while above threshold some nonlinearities have to be postulated (Julesz 1980; Sagi and Hochstein 1983, 1985). The general validity of the linear filter based model is also supported by electrophysiological studies reflecting properties of single cortical cells (Marcelja 1980; Daugman 1980). The model examined here performs surprisingly well on all patterns examined except one, which, as can be seen from Fig. 5, (pattern no. 4), contains terminators. There is a very high correlation between human

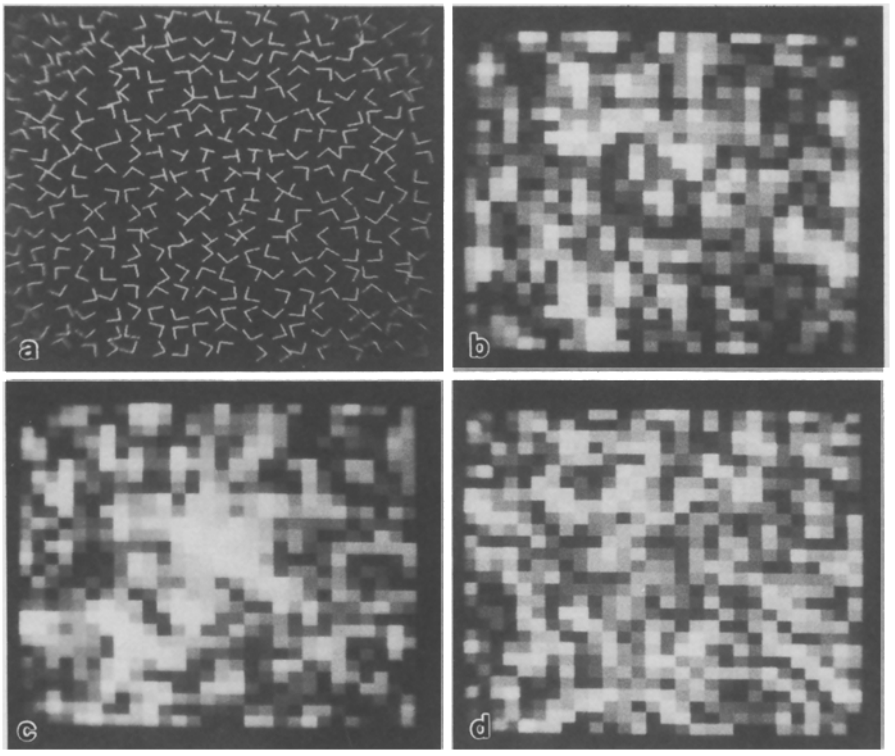

Fig. 10. **a** The input texture pair: *Ts* embedded in *Ls* distractors. **b** The result of convolving Gabor filter with the image ($w=1$, $\theta=90°$). **c** The result for the same frequency when $\theta=45°$. **d** The result of $w=0.625$ and $\theta=90°$

performance and the model performance, $r=0.96$ when pattern 4 is not considered ($r=0.71$ with pattern 4). In the light of the model's good performance, the failure on terminators deserves special attention. This failure is not totally unexpected, since textures composed of patterns used in pair 4 were shown to have identical power spectrum (Julesz and Caelli 1979). Our model computes local power spectrum and thus may provide useful local information for discrimination on pair 4. Thus we may not be forced to account for terminator detection by adding a special "terminator detector" to the Gabor filter model. A natural extension of the present model, that can give a better discrimination of pair 4, is a model utilizing second order statistics of filter responses (across orientation or space). Similarly, discrimination on pair 4 can be improved by introducing a strong nonlinearity at the filters' outputs. However, more experimental exceptions have to be found before any of this accounts can be implemented.

Another problem to the linear filtering approach is a demonstration by Julesz and Krose (1988) where they show that texture discrimination between textures made of *Ls* and *Xs* is possible even when the relevant spatial frequencies (according to the filtering approach) are missing. That *Xs* and *Ls* can be discriminated by the Gabor filter model is clear from the fact that the datum point relating to *X*/*L* discrimination falls along the same line as the other data points shown in Fig. 5, and from the fact that the GGL algorithm presented here show a good segregation. It is also known that *X*/*L* discrimination depends on the size of the *Xs* and when the *Xs* are made larger, discrimination is reduced (Bergen and Adelson 1988; Voorees and Poggio 1988). However, as Julesz and Krose (1988) points out, it is not clear whether their own demonstration argues against a specific linear-filter based model (laplacian of gaussian) or against the use of linear-filters in general. The assumption that the removal of certain frequencies from the input image results their removal from the output of the linear filters, is not necessarily true, simple nonlinearities as thresholding (or squaring) may introduce them back into the filters outputs. In our model this kind of nonlinearity (squaring) exists, thus the filtered image, after the nonlinearity, will contain frequencies related to the size of the *X* and *L* micropatterns. This filtered image can be segregated by stages *B*–*F* in the GGL algorithm which essentially are performing additional filtering (using a Laplacian of Gaussian). The interesting point here is that in this case the algorithm's output is a map with different gray levels corresponding to the different textures, while in the simple case (non-filtered original images) the output is a map describing the borders between the segregated areas. Although this explanation for the Julesz and Krose (1988) phenomena is speculative, it can be tested psychophysically. Evidence for the essential part of it, the secondary filtering stage, already exists (Sagi and Hochstein 1985; Sagi 1989).

In the GGL algorithm the parameters are set to certain values. The size of the Gaussian envelope is held constant for all frequencies and orientations, which has the effect of decreasing the bandwidth of the filter with increasing frequency. This makes the computation and the comparison between different frequency filters easier. For many images a small variation in the filter size or the Gabor envelope size did not produce any significant difference in the segregation results. In addition it was found that the discrimination ability did not depend critically on a specific frequency or orientation. In some cases the combination of several filters produces a better discrimination. The necessity of step D in the GGL algorithm depends on the size of the smoothing operation: the larger the smoothing spread the less the noise. On the other hand the borders become less and less accurate, so for high resolution borders step D is necessary and for lower resolution it can be bypassed while increasing the smoothing operation scale. We used the isotropic Laplacian filter to find the borders in all directions. The Laplacian step comes after thresholding the image. These steps can be interchanged and in that case an algorithm for skeletoning the picture is needed after thresholding. We checked an iterative version of the GGL algorithm and found that the borders between different textures become less accurate. Turner (1986) used Gabor filters iteratively and could discriminate well even texutres with identical third order statistics. Nothdurft (1985) and Sagi and Julesz (1987) have shown that texture discrimination is highly dependent on the density of the input micropatterns within the image. Denser texture leads to higher discrimination. The performance of our model improves when the density of the texture elements is being increased.

We can summarize these results and conclude that: *(1)* Visual discrimination performance is continuous in the sense that discriminative ability increases with the differences between the micropatterns. *(2)* The human visual system can be divided into preattentive/attentive modes, by introducing a threshold range that separates the parallel and sequential modes. Similarity values around the threshold may produce preattentive detection depending on stimulus configuration, and noise level. Practically, this means that stimuli having discriminability values within this range can not serve as good indicators for preattentive or attentive processes. *(3)* The filtering approach seems to predict quite accurately human performance in preattentive tasks, and offers some natural ways to accommodate for the unaccountable cases.

Acknowledgements. We would like to thank Nissan Spector and Bart Rubenstein for their helpful comments and help in editing. This work was supported by a grant from the Israel Academy of Sciences and Humanities.

References

Bajcsy R (1973) Computer description of textured surfaces. IJCAI 20–23

Beck J (1972) Similarity grouping and peripheral discriminability under uncertainty. Am J Psychol 85:1–19

Beck J (1983) Textural segmentation, 2nd order statistics, and texture elements. Biol Cybern 48:125–130

Beck J, Sutter A, Ivry R (1987) Spatial frequency channels and perceptual grouping in texture segregation. Comput Vision, Graph Image Proc 37:299–325

Bergen JR, Adelson EH (1988) Early vision and texture perception. Nature (London) 333:363–364

Bergen JR, Julesz B (1983) Parallel versus serial processing in rapid pattern discrimination. Nature 303:696–698

Caelli T, Moraglia G (1985) On the detection of Gabor signals and discrimination of Gabor textures. Vision Res 25:671–684

Daugman JD (1980) Two dimensional spectral analysis of cortical receptive field profiles. Vision Res 20:847–856

Daugman JD (1987) Image analysis and compact coding by oriented 2-D Gabor primitives. SPIE Process 758:19–30

Fairhurst MC, Stonham TJ (1976) A classification system for alphanumeric characters based on learning network techniques. Digital Process 2:321–339

Gabor D (1946) Theory of communication. J IEE (London) 93:429–457

Gurnsey R, Browse RA (1987) Micropattern and presentation conditions influencing visual texture discrimination. Percept Psychophys 41:238–252

Hall EL (1979) Computer image processing and recognition. Academic Press, New York

Julesz B (1962) Visual pattern discrimination. IRE Trans Inf Theory 8:84–92

Julesz B (1975) Experiments in the visual perception of texture. Sci Am 232:34–43

Julesz B (1980) Spatial nonlinearities in the instantaneous perception of textures with identical power spectra. Phil Trans R Soc London B 290:83–94

Julesz B (1981) Textons, the elements of texture perception and their interactions. Nature 290:91–97

Julesz B (1984a) A brief outline of the texton theory of human vision. TINS 7:41–45

Julesz B (1984b) Toward an axiomatic theory of preattentive vision. In: Edelman GM, Gall WE, Cowan WM (eds) Dynamic aspects of neurocortical function. Neurosciences Research Foundation, New York, pp 585–612

Julesz B (1986) Texton gradients: The texton theory evisited. Biol Cybern 54:245–251

Julesz B, Caelli T (1979) On the limit of Fourier decompositions in visual texture perception. Perception 8:69–73

Julesz B, Krose BJA (1988) Features and spatial filters. Nature (London) 333:302–303

Krose BJA (1986) A description of visual structure. PhD thesis, Department of Industrial Design Engineering, Delft University of Technology, The Netherlands

Krose BJA (1987) Local structure analyzers as determinants of preattentive pattern discrimination. Biol Cybern 55:289–298

Marcelja S (1980) Mathematical description of the responses of simple cortical cells. J Opt Soc Am 70:1297–1300

Nothdurft NC (1985) Sensitivity for structure gradient in texture discrimination task. Vision Res 25:1957–1968

Rosenfeld A, Kak AC (1976) Digital picture processing. Academic Press, New York

Sagi D (1988) The combination of spatial frequency and orientation is effortlessly perceived. Percept Psychophys 43:601–603

Sagi D (1989) Hierarchy of spatial filtering in early vision. Invest Ophthalmol Vis Sci [Suppl] 30:234

Sagi D, Hochstein S (1983) Discriminability of superthreshold compound spatial frequency gratings. Vision Res 23:1595–1606

Sagi D, Hochstein S (1985) Lateral inhibition between spatially adjacent spatial frequency channels? Percept Psychophys 37:315–322

Sagi D, Julesz B (1987) Short-range limitation on detection of feature differences. Spatial Vision 2:39–49

Treisman A (1986) Feature and objects in visual processing. Sci Am 255:106–125

Turner MR (1986) Texture discrimination by Gabor functions. Biol Cybern 55:71–82

Voorees H, Poggio T (1988) Computing texture boundaries from images. Nature (London) 333:34–367

Watson AB (1983) Detection and recognition of simple spatial forms. In: Braddick OJ, Sleigh AC (eds) Physical and biological processing of images. Springer, Berlin Heidelberg New York

Wilson HR (1983) Psychophysical evidence for spatial channels. In: Braddick OJ, Sleigh AC (eds) Physical and biological processing of images. Springer, Berlin Heidelberg New York

Received: April 29, 1988

Accepted in revised form: February 2, 1989

Dr. Dov Sagi
Department of Applied Mathematics & Computer Sciences
The Weizmann Institute of Science
Rehovot 76100
Israel